KEK CP-008
KEK Preprint 93-138
October 1993
H

Complete tree level calculation of the process $e^+e^- \to \nu\bar{\nu}b\bar{b}$ and the Higgs signal at LEP200 and Next Linear Colliders

M.Dubinin, V.Edneral
Institute for Nuclear Physics, Moscow State University
119899 Moscow, Russia

Y.Kurihara and Y.Shimizu,
National Laboratory for High Energy Physics (KEK)
Tsukuba, Ibaraki 305, Japan

August 21, 1993

Abstract

We present the results of complete tree level calculation of the process $e^+e^- \to \nu\bar{\nu}b\bar{b}$ at the energies of LEP200 and Next Linear Colliders. Automatic generation of the squared matrix element was carried out by GRACE and CompHEP systems. We study in details the behavior of cross-section as a function of c.m.s. energy and Higgs boson mass. Particularly we point out the possibility of Higgs boson detection at LEP200 energies under the resonance threshold ($\sqrt{s} < m_H + m_Z$). Comparison is made with the effective $2 \to 2$-body approximation for Higgs production. The approximation is satisfactory at LEP200 energies, but at higher energies rather large discrepancy is observed.

Submitted to Physics Letter B.

National Laboratory for High Energy Physics, 1993

KEK Reports are available from:

Technical Information & Library
National Laboratory for High Energy Physics
1-1 Oho, Tsukuba-shi
Ibaraki-ken, 305
JAPAN

Phone: 0298-64-1171
Telex: 3652-534 (Domestic)
(0)3652-534 (International)
Fax: 0298-64-4604
Cable: KEK OHO
E-mail: LIBRARY@JPNKEKVX (Bitnet Address)
library@kekvax.kek.jp (Internet Address)

1 Introduction

Within the framework of Standard Model[1] the mass of Higgs boson can take an arbitrary value. Experimentally LEP100 data settled the lower limit of the mass around 60 GeV [2]. The region above 60 GeV will be covered by the LEP200 collider. The best possibilities for the discovery of heavy Higgs particle ($m_H > 2m_Z$) will be probably given by the future hadronic colliders LHC and SSC[3]. However, these machines are not suitable for the detection of the intermediate mass Higgs (100 GeV $< m_H < 2m_Z$) due to large hadronic backgrounds. Next Linear Colliders (NLC) with e^+e^- beams will have undoubtedly better possibility because of less backgrounds.

Existing calculations for LEP200 are based on the approximation based on the $2 \to$ 2-body reactions[4] for the signal process(Higgs bremsstrahlung from Z boson line[5])

$$e^+e^- \to HZ \tag{1}$$

and for the main background reactions

$$e^+e^- \to ZZ, \quad e^+e^- \to \gamma Z, \quad e^+e^- \to \gamma\gamma \tag{2}$$

where the final particles can be off-shell. Numerical simulations for the bremsstrahlung process Eq.(1) with the backgrounds Eq.(2) using standard PYTHIA 5.6 /JETSET 7.3 package [6] were presented for instance in Ref.[7]. Light Higgs boson has the dominant decay mode $H \to b\bar{b}$, so the realistic event signatures could be observed in the final states $e^+e^-b\bar{b}, \mu^+\mu^-b\bar{b}$, $\tau^+\tau^-b\bar{b}$, $\nu\bar{\nu}b\bar{b}$ and $2jet + b\bar{b}$.

In these calculations the signal and the main background diagrams are considered separately, that is, the incoherent sum is taken. Also some additional background processes besides (2) are not taken into account. However, the contributions from the interference terms and the additional backgrounds could be not so small to neglect. It is interesting to find out if such approximation is satisfactory for the high statistics NLC experiments. In order to understand the limits of applicability of the $2 \to$ 2-body approximation, it is necessary to perform complete tree level calculations for the $2 \to$ 4-body processes including all possible diagrams.

There are several examples of the complete tree level calculations for the Higgs production approximated by the $2 \to$ 3-body processes. The most detailed are the calculations for $e^+e^- \to \nu\bar{\nu}H$[8]. This reaction cannot be

considered as a trivial extension of the $e^+e^- \to Z^*H \to \nu\bar{\nu}H$ when $\nu = \nu_e$, because in this case the t-channel $WW \to H$ fusion signal diagram appears. The contribution of this diagram is important not only at high energies $\sqrt{s} \sim$ 500 GeV where the fusion mechanism dominates over the bremsstrahlung mechanism, but also under the Z resonance threshold[9]. When the mass of the Higgs is sufficiently high to restrict kinematically the production of the on-shell Z, $m_H > \sqrt{s} - m_Z$, the fusion mechanism is the main one. It is interesting to notice that this is not the case for $e^+e^- \to e^+e^-H$ channel because the contribution from $ZZ \to H$ fusion diagram is canceled by the negative interference term among the bremsstrahlung and fusion diagrams.

Another example of the complete tree level calculation in the $2 \to$ 3-body process for the Higgs production is $e^+e^- \to Zb\bar{b}$ considered in Ref.[9]. This case is again not a trivial extension of the $e^+e^- \to ZH^* \to Zb\bar{b}$ process because it includes additional background diagrams (for instance, Z emission from the b-quark line). All interference terms were taken into account (9 diagrams, 45 squared diagrams). The correction to the $2 \to$ 2-body approximation is small but not negligible(several % to σ_{tot}, 10 % to the $b\bar{b}$ mass distribution). This process should be equivalent to $e^+e^- \to \mu^+\mu^-b\bar{b}$ process with the stringent kinematical cut for the $\mu^+\mu^-$ invariant mass. In order to know how this cut suppresses the cross section, a calculation was done in Ref.[10] with the complete set of $2 \to 4$ diagrams giving the $\mu^+\mu^-b\bar{b}$ final state in the whole physical region of phase space in tree approximation, by taking into account all possible contributions (25 diagrams, 595 squared diagrams).

In this paper we consider the possibility of Higgs boson detection in the process $e^+e^- \to \nu\bar{\nu}b\bar{b}$, assuming that the signal is reconstructed in the invariant mass distribution of two b-jets. The advantages of this channel are, as we shall see, in the fact that the cross section, which is increasing with energy, is larger at LEP200 energies than in the case of $\mu^+\mu^-b\bar{b}$ channel.

2 Higgs signal in the $e^+e^- \to \nu\bar{\nu}b\bar{b}$ process

We represent 23 Feynman diagrams corresponding to the $e^+e^- \to \nu_e\bar{\nu}_eb\bar{b}$ process in the tree approximation in Fig.1. The first row shows two signal diagrams, the bremsstrahlung diagram and the fusion diagram. The second and the third rows contain the main background diagrams. The fourth

row includes multiperipheral type diagrams with charged current transitions between quarks. Only the first diagram in this row(with the intermediate top quark) can contribute, as two others are suppressed by CKM mixings. The fifth row represents t-channel W-exchange diagrams. The sixth and the seventh rows show s-channel background diagrams. In comparison with the $\mu^+\mu^- b\bar{b}$ final state we have one additional signal diagram and two types of new diagrams for the background(W-exchange and multiperipheral).

The generation of the diagrams, calculation of the matrix element squared and generation of the optimized FORTRAN code were performed independently by means of two integrated systems for automatic calculations – GRACE v. 1.0 [11] and CompHEP [12] v.2.51c(C version for workstations). The following Monte-Carlo integration over the phase space was done with the help of BASES package[13].

We used the Breit-Wigner propagators for the Higgs and Z bosons in the intermediate states. There are no divergent diagrams in the whole set, so it is possible to calculate without kinematical cuts. The total cross-section for the $e^+e^- \to \nu_e\bar{\nu}_e b\bar{b}$ process is shown in Fig.2. Some nontrivial structure in the behavior of σ_{tot} appears due to the existence of two main mechanisms for the Higgs production, giving different energy dependence. In comparison with the $e^+e^- \to \mu^+\mu^- b\bar{b}$ case[10] the $\nu_e\bar{\nu}_e b\bar{b}$ channel has the cross-section 2–3 times larger at $\sqrt{s} = 200 - 300$ GeV and increasing at higher energy, while the $\mu^+\mu^- b\bar{b}$ cross-section decreases. At $\sqrt{s} = 190$ GeV $\sigma_{tot}(e^+e^- \to \nu_e\bar{\nu}_e b\bar{b})$ is 3.6 times larger if the Higgs boson with the mass $m_H = 80$ GeV exists and 1.52 times larger if $m_H = 100$ GeV compared with the case of no Higgs. It follows that simple counting rate with the σ_{tot} could show the Higgs signal.

The total cross-section for all possible types of neutrino(ν_e, ν_μ, ν_τ) changes the result for ν_e only at the energies above the HZ threshold. In the case of muon and tau neutrino there is no fusion mechanism and at high energies the contribution of these channels decreases(Fig.2). For the same reason they are not important at the energies below the threshold.

The reduction of the background from hadronic jets can be made by widely discussed b-tagging procedure(for instance, Ref.[14]) that gives the possibility to distinguish the b-quark jets from light quark jets. We are not going to discuss here the experimental restrictions imposed by b-tagging. We like to notice that the direct reconstruction of two b-jets allows one to use high efficiency(80% and more) tagging regime when the probability of double misidentification of some particles(for instance, c-quarks) as the b-quarks is very low.

The background coming from the process $e^+e^- \to e^+e^- b\bar{b}$ is large. The total cross-section can be about two orders of magnitude larger than $\nu_e\bar{\nu}_e b\bar{b}$. However the dominant part of the background corresponds to the case when electron and positron scatter in forward-backward directions. This background can be therefore reduced by electron veto in the detector and requirement of the sufficient missing mass for the b-jets.

We show the dependence of $\sigma_{tot}(e^+e^- \to \nu_e\bar{\nu}_e b\bar{b})$ on the Higgs mass in Fig.3. At the energy $\sqrt{s} = 500$ GeV the cross section with 140 GeV Higgs boson is about half of that with 80 GeV Higgs boson.

In Fig.4 we show the $b\bar{b}$ mass distributions at the c.m.s. energies greater than the resonance threshold $\sqrt{s} > m_H + m_Z$ for different Higgs masses. In this case the Higgs signal is rather clean. It is interesting if one can see the top signal below the open $t\bar{t}$ threshold(for instance in the case $\sqrt{s} = 300$ GeV, $m_{top} = 150$ GeV). Unfortunately the top signal seems to be much smaller than the background from W-exchange diagrams.

The most interesting case is shown in Fig.5, where we represent the cross sections for the case $\sqrt{s} < m_H + m_Z$ at LEP200 energies. Here both Higgs and Z cannot be produced on mass-shell and the dominant contribution in the case of $\nu = \nu_e$ comes from the second signal diagram in Fig.1(fusion diagram). Having 0.5 fb -1 data accumulation, one can expect from 2 to 6 signal events at the Higgs masses 100–110 GeV below the resonance threshold before any experimental cuts. In the Table below the areas of the Higgs peak in Fig.5 are denoted as σ_{Higgs} and the corresponding numbers of expected events are summarized.

We considered the simplified case with no cuts and the initial radiation being switched off. If these factors do not influence significantly on the result, the $\nu_e\bar{\nu}_e b\bar{b}$ channel gives the possibility to detect the Higgs signal or to set the lower limit of the Higgs mass around 100 GeV at $\sqrt{s} = 180$ GeV and around 105–110 GeV at $\sqrt{s} = 190 - 200$ GeV. Of course, more realistic simulation should be done to ascertain this conclusion. The problem of backgrounds is very important when the possible number of events is small.

$\sqrt{s}$ GeV	m_H GeV	σ_{tot} fb	σ_{Higgs} fb	Number of expected events
180	100	9.4	5.0	2.5
190	100	31.2	11.2	5.6
190	110	24.5	4.2	2.1
200	110	36.7	9.3	4.7
200	120	30.9	3.6	1.8

3 The contribution of additional backgrounds and interference terms

The usual way to simulate the Higgs signal Eq.(1) and the main background Eq.(2) in $2 \to$ 2-body approximation is to take into consideration the bremsstrahlung signal diagram and four main background diagrams(second row in Fig.1). Off-shell Higgs and Z bosons then decay into $b\bar{b}$ and $\nu\bar{\nu}$. Such procedure leads to some underestimation of the signal and background especially at the energies below the threshold $\sqrt{s} < m_H + m_Z$ and at higher energies, when the contributions of neglected diagrams are not small.

In order to understand the possible difference from the complete calculation in the case when both brmsstrahlung and fusion mechanisms contribute, let us consider only the diagrams from the first three rows in Fig.1 and compare with the signal and main background in the same way used in [10]. Here the interference terms are retained only if they have the same intermediate 2-body state(improved $2 \to$ 2-body approximation). In contrast to the usual approximation we integrated over the whole four particle final state instead of usual integration over two particle phase space followed by $1 \to 2$ decay. The relative difference is expressed by the ratio

$$\Delta\sigma = \frac{\sigma_{ctl} - \sigma_{appr}}{\sigma_{ctl}} \times 100\% \qquad (3)$$

In this formula σ_{ctl} denotes the complete tree level value (for σ_{tot} or $d\sigma_{tot}$ in the given bin for invariant mass) and σ_{appr} denotes the value in the approximation we have described.

Our calculation shows that the value of $\Delta\sigma$ for the total cross section is increasing with energy. It is about 0.8% for $\sqrt{s} = 200$ GeV, $m_H = 80$ GeV and about 8% for $\sqrt{s} = 500$ GeV, $m_H = 140$ GeV. A variation of 8% in $\Delta\sigma$ corresponds to 100 events at the NLC luminosity of $10fb^{-1}$ and is rather remarkable. It is due to the increasing role of multiperipheral and W-exchange diagrams(fourth and fifth rows in Fig.1). In the $\mu^+\mu^- b\bar{b}$ channel[10] $\Delta\sigma$ is 0.2% in the case $\sqrt{s} = 200$ GeV, $m_H = 80$ GeV and no difference is observed at all at 500 GeV as W-exchange diagrams are absent in this case.

The result of $\Delta\sigma$ calculation for the invariant $b\bar{b}$ mass distribution is shown in Fig.6. The values of invariant mass for the complete tree level case are regularly smaller than those in approximated calculation. The maximum difference in a bin can reach more than 7% at low $M_{b\bar{b}}$(for $\sqrt{s} = 500$ GeV). It follows that the approximate calculation is rather good at LEP200 energies, but for NLC it is not satisfactory. In particular, large deviations can take place in the angular distribution of forward-backward b-jets and missing mass distributions.

4 Conclusion

In this paper we presented the results of the complete tree level calculation for the $2 \to 4$ process $e^+e^- \to \nu_e\bar{\nu}_e b\bar{b}$(23 diagrams in the unitary gauge) in the Standard Model. We considered the possibility to detect the Higgs signal through this reaction at LEP200 and Next Linear Colliders. The distinguishing feature of the $\nu_e\bar{\nu}_e b\bar{b}$ channel is the presence of the fusion diagram for the signal(Fig.1), giving large contribution not only at the energies $\sqrt{s} > 0.5$ TeV but also at the energies below the resonance threshold ($\sqrt{s} < m_H + m_Z$) typical for the LEP200 energy range in the case of relatively light Higgs. Some new features are introduced by the W-exchange diagrams and ladder diagram with intermediate t-quark.

Total cross-section of the process $e^+e^- \to \nu_e\bar{\nu}_e b\bar{b}$ is $2-3$ times larger than that for the $e^+e^- \to \mu^+\mu^- b\bar{b}$ process at LEP200 energies and increasing with energy. The detection of the Higgs signal can be made by the direct reconstruction of the two b-jets in the case of high efficiency b-tagging. The background from $e^+e^- b\bar{b}$ channel can be reduced by electron veto in the detector and triggering with sufficient missing mass.

Fusion mechanism for the Higgs production gives the possibility to ob-

serve signal at the energy below the resonance threshold(see the Table). An estimation of the number of events shows that we can find the signal for Higgs with m_H around $105 - 110$ GeV at the energies $180 - 200$ GeV. This distinguished property of the $\nu_e\bar{\nu}_e b\bar{b}$ channel allows to observe at LEP200 energies the Higgs boson with the mass of about 10 GeV larger than expected from the previous study.

We investigated also the validity of improved $2 \to 2$-body process taking into account only two signal diagrams with interference between them and the main background diagrams with interference terms between the diagrams containing the same intermediate two particle state. At LEP200 energies such approximation is satisfactory but at higher energies the error of the approximation increases(giving about 10% discrepancy with the exact tree level result at $\sqrt{s} \sim 500$ GeV). This example shows that one should be very careful to use effective approximations and in our case it is not clear at all how to find satisfactory higher energy approximation.

We would like to notice that our study is based on tree level calculation and in this sense is restricted. Some corrections to the results will arise from radiative corrections, detector cuts, simulation of b-jets, efficiency of b-tagging and event reconstruction in the real experiment.

Acknowledgements

M.D. is grateful to E.Boos and S.Shichanin for useful discussions. M.D. and V.E. would like to express their gratitude to V.Ilyin and A.Pukhov for the help with CompHEP system, and Y.K. and Y.S. to T. Kaneko, S. Kawabata, H. Tanaka and T. Ishikawa for the GRACE system. Authors are indebted to Japanese companies KASUMI Co. Ltd and SECOM Co. Ltd. for the financial support and understanding of our work.

References

[1] S.L.Glashow Nucl.Phys., 22 (1961) 579
A.Salam, in: Elementary Particle Theory, ed.by N.Svartholm, Almquist and Weksell, Stockholm, 1968, p.367
S.Weinberg Phys.Rev.Lett., 19 (1967) 1264

[2] L3 collaboration, CERN preprint CERN-PPE/93-31, 1993
S.C.C.Ting, CERN preprint CERN-PPE/93-34, 1993

[3] Proc. of the ECFA Large Hadron Collider Workshop, ed by G.Jarlskod and D.Rein, CERN report 90-10, Geneva, 1990, vol.II, p.427
J.F.Gunion,G.L.Kane, in: Research Directions for the Decade (Proc. of the 1990 Summer Study on High Energy Physics, Snowmass), ed.by E.L.Berger and I.Butler, World Scientific, Singapore, 1991, p.59

[4] S.L.Wu et.al., in: Proc. of the ECFA Workshop on LEP200, ed.by A.Bohm, W.Hoogland, CERN report 87-08, 1987, p.312
Z.Kunszt, W.Stirling Phys.Lett., 242B (1990) 507
N.Brown Z.Phys., C49 (1991) 657
P.Janot, in:'92 Electroweak Interactions and Unified Theories (Proc.of the XXVII Recontre de Moriond), ed.by Tran Than Van, Editions Frontieres, 1992, p.317
JLC group, KEK report 92-16, 1992

[5] J.D.Bjorken, in: Proc. of the 1976 SLAC Summer Institute on Particle Physics, ed.by M.Zipf, Stanford, 1976, p.1
J.Ellis, M.K.Gaillard, D.V.Nanopoulos Nucl.Phys., B106 (1976) 292
B.L.Ioffe, V.A.Khoze Phys.of Elem.Part. and At.Nucl.(USSR), 9 (1978) 118

[6] T.Sjoestrand, PYTHIA 5.6 and JETSET 7.3, CERN preprint-TH.6488/92, 1992

[7] P.Grosse-Wiesmann, D.Haidt, H.J.Schreiber, in: e^+e^- collisions at 500 GeV: the physics potential, ed.by P.Zerwas, DESY report 92-123A, 1992, p.37

[8] R.N.Cahn, S.Dawson Phys.Lett., 136B (1984) 196
K.Hikasa Phys.Lett., 164B (1985) 341
M.S.Chanowitz, M.K.Gaillard Nucl.Phys., B261 (1985) 379
G.Altarelli, B.Mele, F.Pitolli Nucl.Phys., B287 (1987) 205
G.L.Kane, J.Scanio Nucl.Phys., B291 (1987) 221
Y.Kurihara, in: Proc. of the First Workshop on JLC, ed.by S.Kawabata, KEK report 90-2, 1990, p.195

[9] E.E.Boos, M.N.Dubinin, preprint INP MSU 92-41/290, 1992
E.E.Boos, M.N.Dubinin Phys.Lett., B308 (1993) 147

[10] E.Boos, M.Sachwitz, H.J.Schreiber, S.Shichanin, DESY preprint, to be published, 1993.

[11] T.Ishikawa, T.Kaneko, K.Kato, S.Kawabata, Y.Shimizu, H.Tanaka. GRACE manual, KEK report 92-19, 1993

[12] E.Boos et.al.,in: '91 Electroweak Interactions and Unified Theories (Proc. of the XXVIth Recontre de Moriond), ed.by J.Tran Than Van, Editions Frontieres, 1991, p.501
E.Boos et.al.,in: New Computing Techniques in Physics Research II (Proc. of the Second Int.Workshop on Software Engineering, Artificial Intelligence and Expert Systems in High Energy and Nuclear Physics), ed.by D.Perret-Gallix, World Scientific, 1992, p.665

[13] S.Kawabata Comp.Phys.Comm., 41 (1986) 127

[14] H.Borner, P.Grosse-Wiesmann, in: e^+e^- collisions at 500 GeV: the physics potential, ed.by P.Zerwas, DESY report 92-123A, 1992, p.63

Figure captions

Fig.1 Feynman diagrams for the process $e^+e^- \to \nu_e\bar{\nu}_e b\bar{b}$.

Fig.2 Total cross-section for the processes $e^+e^- \to \nu_e\bar{\nu}_e b\bar{b}$ and $\nu_\mu\bar{\nu}_\mu b\bar{b}$ vs. energy. We use the following parameters: $m_b = 5.0$ GeV, $m_{top} = 150$ GeV, $m_Z = 91.16$ GeV, $\Gamma_Z = 2.53$ GeV, $m_c = 1.35$ GeV, $\sin\theta_w = 0.475$, and $e = \sqrt{4\pi\alpha} = 0.313$. The widths of Higgs boson are 4.41, 5.55, 6.69 and 7.83 MeV for the masses 80, 100, 120 and 140 GeV, respectively.

Fig.3 The Higgs mass dependence of the total cross-section of $e^+e^- \to \nu_e\bar{\nu}_e b\bar{b}$ for various c.m.s. energies.

Fig.4 The $b\bar{b}$ mass distribution for LEP200 energy region higher than the threshold($\sqrt{s} > m_H + m_Z$) with several Higgs masses. The peaks around $M_{bb} \sim 90$ GeV are the Z and others are Higgs.

Fig.5 The $b\bar{b}$ mass distribution for LEP200 energy region less than the threshold($\sqrt{s} < m_H + m_Z$) with several Higgs masses. The small bump in a) and solid lines in b) and c) around $M_{bb} \sim 90$ GeV are the Z peak. Other peaks correspond to Higgs signal.

Fig.6 The difference $\Delta\sigma$ in % between exact calculation and approximation(see the formula Eq.(3)).

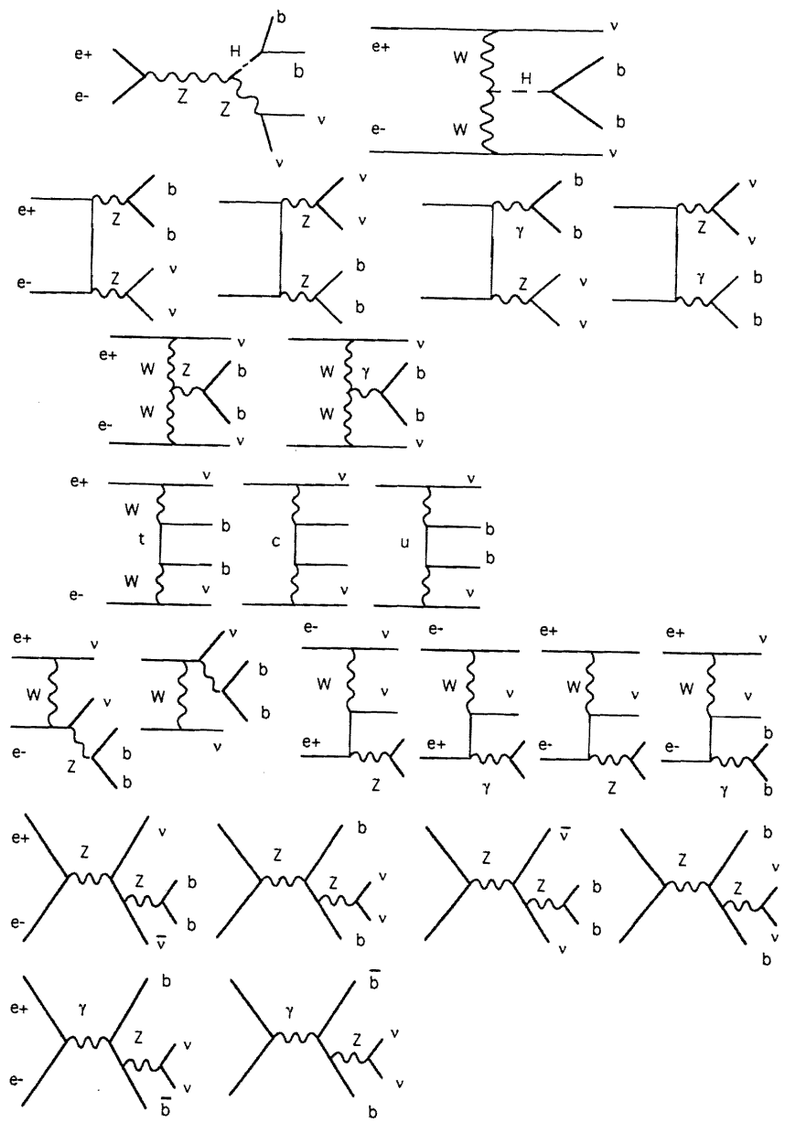

Figure 1

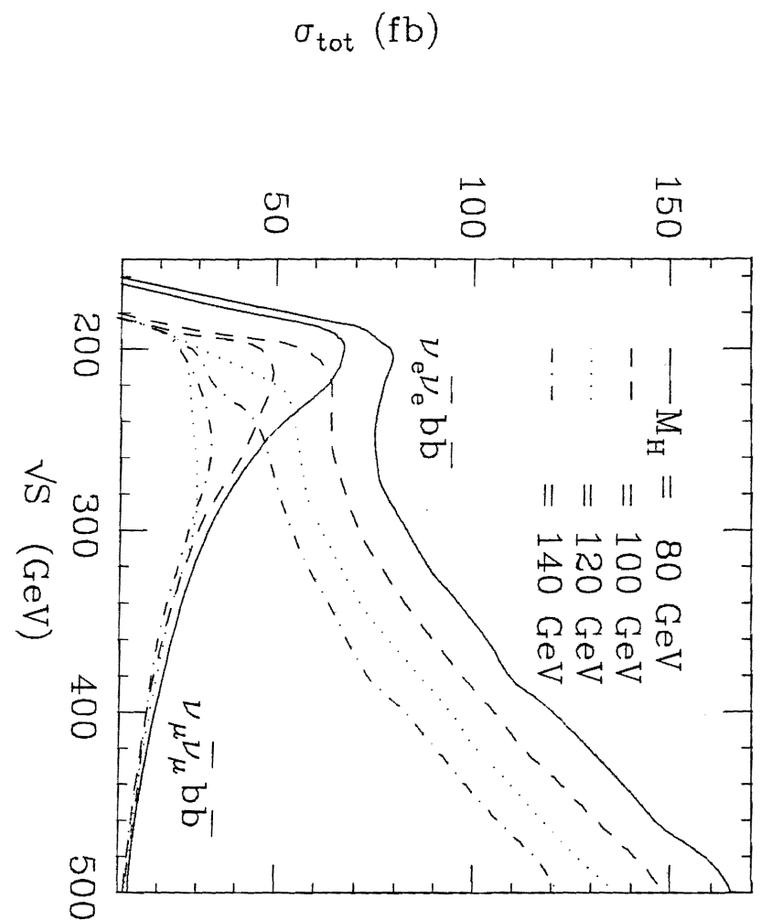

Figure 2

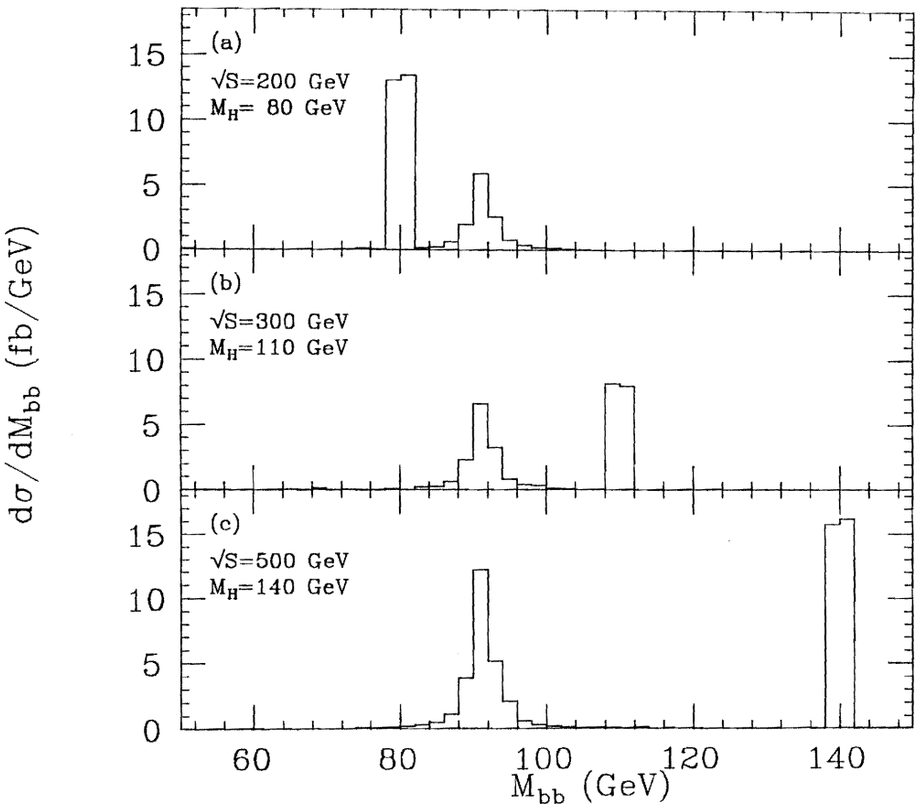

Figure 4

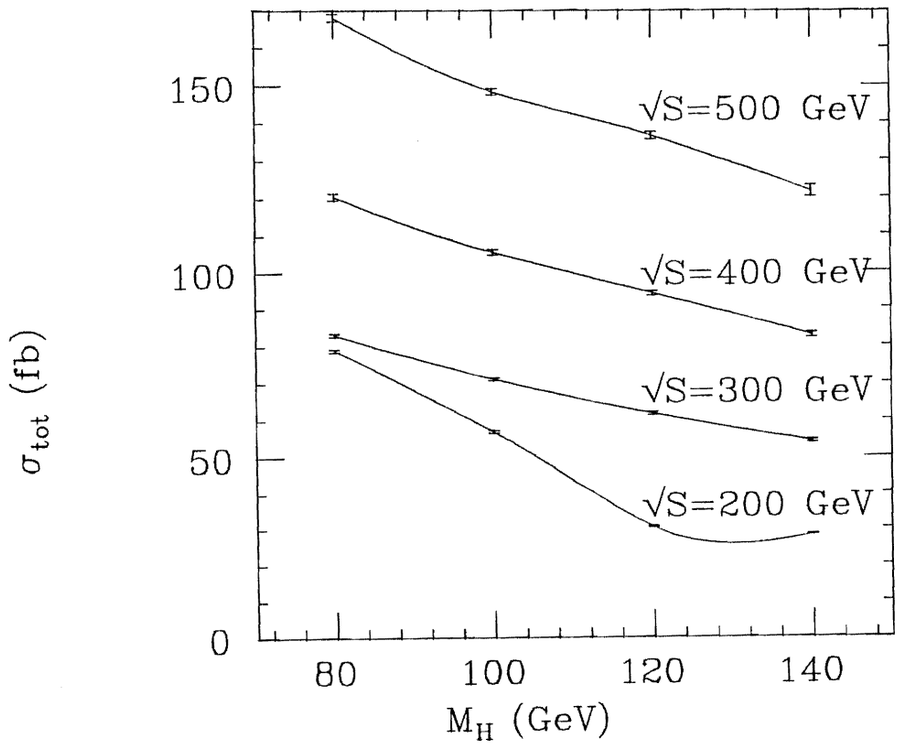

Figure 3

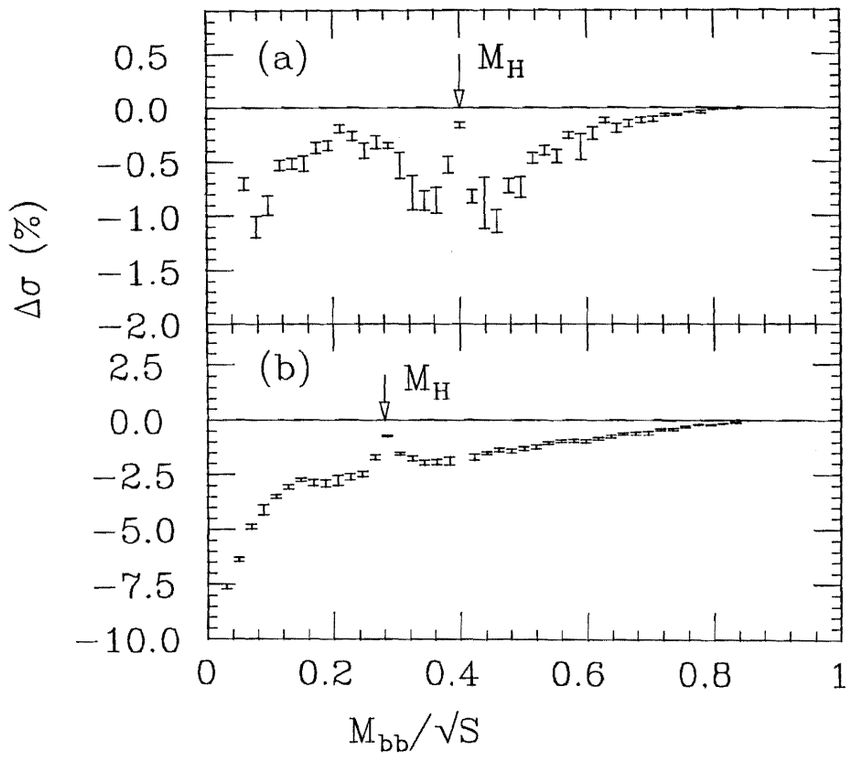

Figure 6

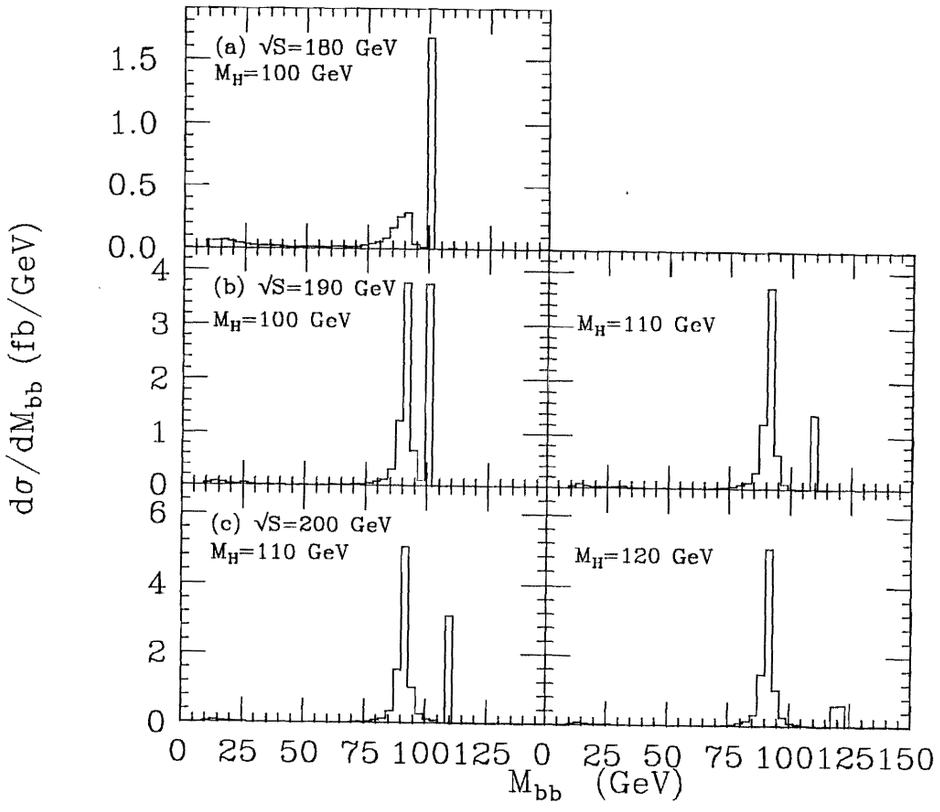

Figure 5